Waveguiding by Axicon-Focused Laser Beams

I.V.Pogorelsky
Brookhaven National Laboratory
ATF - Bldg. 820, Upton, NY 11973
W.D.Kimura
STI Optronics, Inc.
2755 Northup Way, Bellevue, WA 98004
Y.Liu
UCLA Department of Physics
Los Angeles, CA 90024

Abstract

We propose a method for formation of a long plasma waveguide based on axicon focusing of a radially polarized CO_2 laser pulse into a uniform, low density discharge plasma. Simulations demonstrate that an extended cylindrical plasma channel with a wall height $\Delta N_e = 1.5 \times 10^{16} cm^{-3}$ will be produced in a DC or RF discharge in 0.17 atm of hydrogen after axicon-focusing of a nanosecond 1-GW/cm^2 CO_2 laser pulse.

1. Introduction

With contemporary terawatt picosecond lasers, extremely high intensity levels, $10^{16} - 10^{18} W/cm^2$, are attainable upon the tight focusing of laser beams. The transverse electric field corresponding to such intensities is 3-30 GV/cm. Several schemes based on resonance coupling of laser radiation into plasma waves are under development to convert a portion of this enormous field into a longitudinal acceleration field formed by periodic electron-ion space charge separation. Recently demonstrated high-gradient electron acceleration ($\sim 20 MeV/cm$) using laser wake-field[1] and plasma beat-wave[2,3] techniques promises to further advance plasma-based laser accelerator (PBLA) concepts towards practical devices. However, a major limitation with these schemes is the short interaction region in which the required high laser intensity must be maintained. The length of this region is basically equal to the Rayleigh distance, z_0, measured from the focal point to the point where the laser beam expands two times in cross-sectional area. For Gaussian beams, z_0 is intimately related to the waist radius, w_0, by the ratio

$$z_0 = \frac{\pi w_0^2}{\lambda}. \qquad (1)$$

For typical parameters $\lambda = 1 \mu m$ and $w_0 = 50 \mu m$, which means $z_0 = 8 mm$. This restricts the energy gain attainable in a single-stage PBLA driven by a terawatt-class laser to $\sim 100 MeV$. To reach the next milestone of 1 GeV acceleration, far more powerful lasers and/or longer interaction regions would be needed. However,

extremely high laser power (e.g., petawatt) with 1 TV/cm electric fields may be more destructive than productive for plasma-based accelerators due to pondermotive blow out of the plasma from the Rayleigh region[4].

Another possible way to increase the net acceleration without scaling up the drive laser power is optical guiding. A conventional solid waveguide will not withstand intensities at the level of $10^{16}W/cm^2$. The overdense plasma formed in the bulk or at the surface of a solid material will block the radiation path through the waveguide and probably damage it. Considerably more realistic optical guiding options, possibly applicable for PBLA, include: self-focusing due to thermal, nonlinear, pondermotive, and relativistoc effects;[5,6] gas jets;[7] and preformed plasma density channels.[6,7] The latter concept looks promising for producing stable waveguiding conditions. This approach is based on changing the refraction index due to a plasma density gradient according to the equation

$$\frac{\Delta n}{n_0} = -\frac{\Delta N_e}{2N_{cr}}, \tag{2}$$

which follows from $n = n_0\sqrt{1 - \frac{N_e^2}{2N_{cr}^2}}$, where $N_{cr} = \frac{\pi mc^2}{e^2\lambda^2}$.

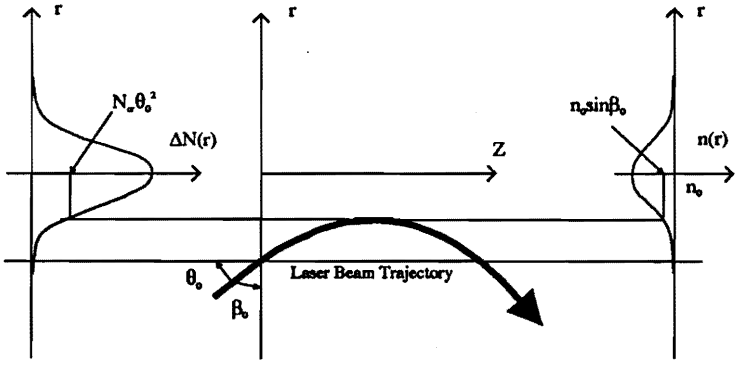

Figure 1: Optical ray trajectory in a plasma layer with a radial density distribution $N_e(r)$ and with corresponding index profile $n(r)$.

For an electromagnetic wave incident onto the plasma layer at an angle β_0 as shown in Fig. 1, the condition for refraction is

$$n(r) \leq n_0 sin\beta_0, \tag{3}$$

or for oblique incidence $n(r) - n_0 \equiv \Delta n(r) \leq -n_0\theta_0^2/2$, and by Eq.(2)

$$\Delta N_e \geq N_{cr}\theta_0^2. \tag{4}$$

If we consider a cylindrical plasma layer, for a focused Gaussian beam with a diffraction divergence of

$$\theta_0 = \frac{\lambda}{\pi w_0} \tag{5}$$

the condition for optical guiding is

$$\Delta N_e \geq \frac{mc^2}{\pi e^2 w_0^2} \equiv (\pi r_e w_0^2)^{-1}. \tag{6}$$

Note that this condition does not depend upon the laser wavelength. For example, a Gaussian laser beam focused into a spot with a radius of $w_0 = 100\mu m$ will be trapped in a plasma waveguide with a "wall height" of $\Delta N_e = 1.5 \times 10^{16} cm^{-3}$.

Optical guiding in a plasma channel over several Rayleigh lengths has been recently experimentally demostrated.[8] The axicon-focused 100-ps Nd:YAG pulse ignited a cylindrical shock wave via optical gas breakdown. The waveguiding properties of the plasma channel inside the shock wave were demonstrated by focusing a delayed portion of the same laser pulse at the entrance of the expanding plasma cylinder and observing the channeled radiation emerging from the other end. This method capitalizes on the axicon (conical lens or mirror) property to concentrate a linear polarized laser beam into a $J_0(2\pi\theta_a r/\lambda)$ radial Bessel distribution extended along the optical axis of the axicon, where θ_a is the double apex angle of the axicon.[9] However, the requirement for optical gas breakdown and shock-wave generation presumes a high laser energy deposition into a gas of relatively high density ($10^{13} - 10^{14} W/cm^2$ laser intensity and Xe gas at 30 Torr were used in the experiment[8]). This may not necessarily correspond to optimum PBLA conditions.

We propose here another method for formation of a long plasma waveguide based on axicon focusing of a short, radially polarized CO_2 laser pulse into a uniform, low density discharge plasma. While requiring a fast discharge driver, the proposed method provides better control of the waveguide parameters, requires relatively low drive power, and may used at lower gas densities closer to optimal PBLA conditions.

2. Generation of radial polarized laser beams

The proposed method is based on the axicon property to produce a $J_1(2\pi\theta_a r/\lambda)$ radial Bessel distribution of the electric field by focusing a radially polarized laser beam in a configuration sketched in Fig. 2.[9] This provides a field profile, naturally shaped with interferometric precision of a cylindrical plasma density distribution appropriate for

waveguiding (see Fig. 3). The process of plasma channel development via electron avalanche multiplication will be considered in the next section. Here we describe a method for generating a radially polarized CO_2 laser beam and its focusing by an axicon mirror, as has been demonstrated during the course of Inverse Cherenkov Acceleration experiments.[10,11]

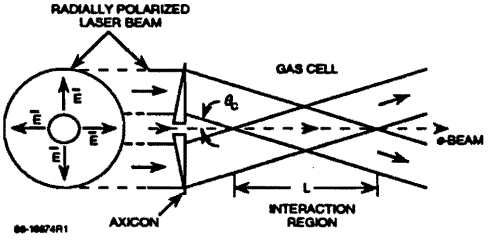

Figure 2: Axicon focusing geometry.

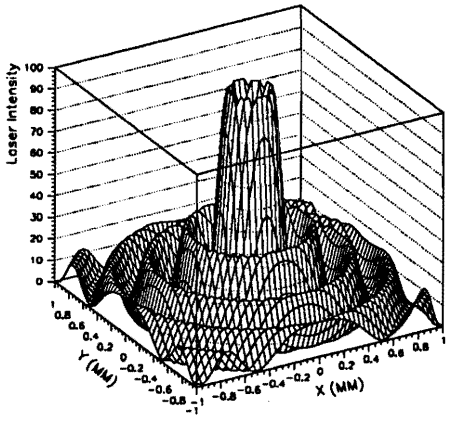

Figure 3: Spatial distribution of a radial polarized laser beam after axicon focusing.

A linearly polarized laser beam is converted into one with radial polarization by using a double interferometer optical set-up as presented in Fig. 4. Key elements of the converter are two spiral phase delay (SPD) plates placed in two legs of the first interferometer stage. The optical thickness increment of the SPD plate along 2π azimuthal rotation is equal to one wavelength for CO_2 laser light. Oriented in opposite directions, these two SPD plates produce clockwise and counter-clockwise spiral wavefronts from the original plane-wave laser beam. The combination of these two counter-rotating wave-fields on a ZnSe 50%-beamsplitter after the first interferometer stage produces a stationary two-lobe azimuthal distribution, in analogy with a stroboscopic effect in mechanics. Actually, the laser beams propagating in the two legs of the second interferometer stage have complementary intensity distributions (TEM_{01} and TEM_{10}). This is the result of a $\pi/2$ phase shift via the reflection at the 50%-beamsplitter at the air/coating surface and a zero-shift due to reflection at the ZnSe/coating surface. After introducing a 90^0 polarization rotation by a conventional $\lambda/2$ retardation plate placed in one leg of the second interferometer, the orthogonally polarized TEM_{01} and TEM_{10} distributions are combined at a polarizing beamsplitter as illustrated by Fig.5. As a result, a radially polarized beam is produced in agreement with the mathematical formalism developed for this type of polarization converter.[10]

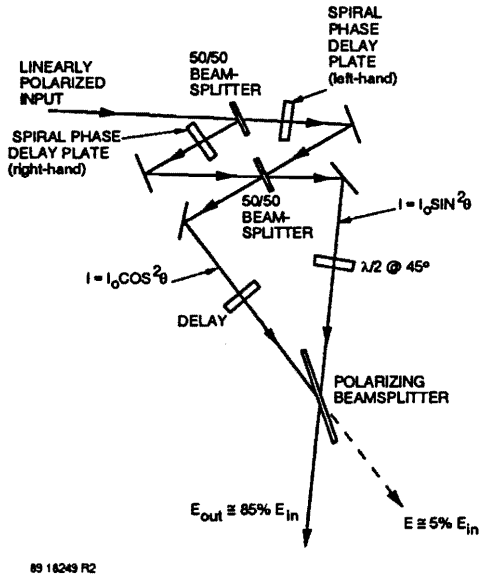

Figure 4: Optical layout for radial polarization converter.

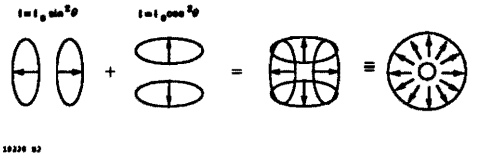

Figure 5: Combination of $sin^2\theta$ and $cos^2\theta$ beams yields radially polarized beam.

When a radially polarized beam is focused by the axicon a circularly symmetric interference pattern is developed along the focal region of the axicon. The analytical solution for the radial component of the electric field $E_r(r,z)$ is a Bessel function of the first kind of order 1:[9]

$$E_r(r,z) = E_0(z) \times J_1(2\pi\theta_a r/\lambda), \tag{7}$$

with $E_0(z)$ is field amplitude depending upon the initial laser intensity distribution at the axicon surface. The radial position of the first maximum in the distribution of Eq.(7) occurs at

$$r_{max} = 0.29\lambda/\theta_a, \tag{8}$$

and is equal to 170 μm for a representative case of $\lambda = 10.6\mu m$ and $\theta_a = 20mrad$.

Neglecting diffraction effects, the distribution $E_0(z)$ along the axicon focal region for a Gaussian input beam described by $P(R) = P_0 exp\{-(2R/\Delta)^2\}$ with $\Delta = 5mm$ (see Fig. 6 a) is shown in Fig. 6 d. In a practice, the axicon would have a hole in the middle to introduce the guided laser beam and/or electron beam for laser acceleration. In order to avoid losses in the center of the axicon-focused beam, the beam can be made annular in shape using an additional axicon telescope. The radial distribution obtained after axicon telescoping of a Gaussian beam is presented in Fig. 6 b. Although it looks quite different from the original distribution presented in Fig. 6 a, axicon focusing of distribution (6 b) results in a similar axial distribution as (6 d), but shifted along the z-axis by the distance equal to the radial expansion of

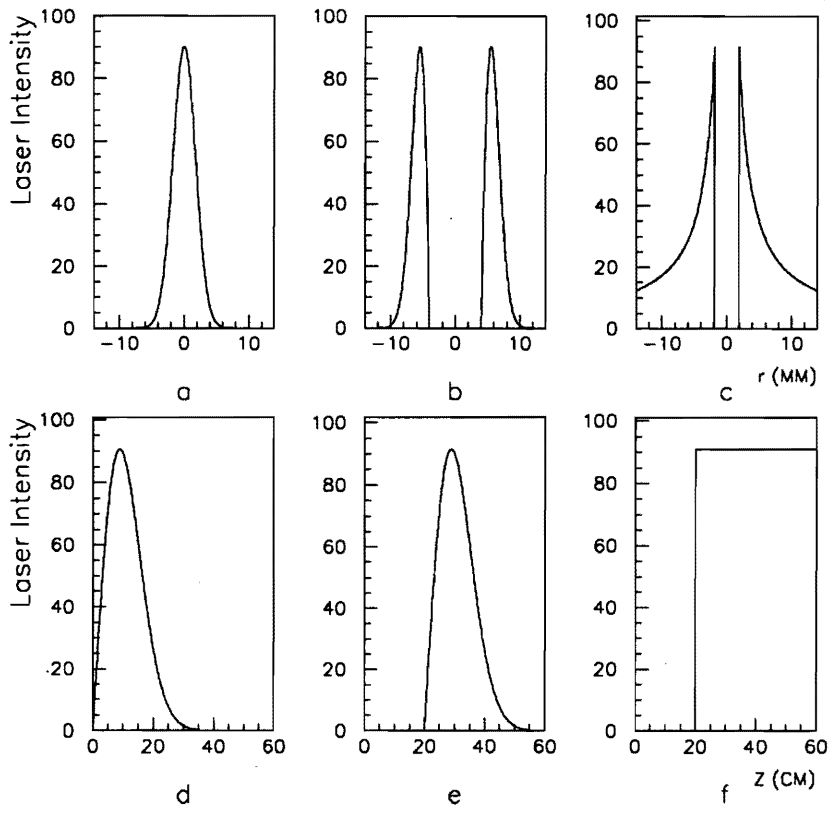

Figure 6: Initial laser beam profiles P(R) with shown below corresponding distributions along the axicon axis $I(z) = z\theta_a P(z\theta_a)$ for $\theta_a = 20mrad$: a) Gaussian beam, b) Gaussian beam axicon-telescoped with radial expansion of $2.5mm$, c) axicon-telescoped hyperbolic beam ($P(R) \sim 1/R$).

the axicon telescope divided by θ_a (compare Figs. 6 d and 6 e). Note, that in order to obtain a constant field amplitude along the z-axis, it would be necessary to tailor the radial field distribution in the way presented in Fig. 6 c.

3. Plasma channel development by avalanche gas breakdown

There are several mechanisms that cause gas breakdown under laser irradiation. At extremely high laser intensities attainable with short picosecond pulses, tunneling and multiphoton ionization are usually the main mechanisms of gas breakdown. The intensity threshold, I_{th}, for these processes depends on the laser wavelength and the ionization potential of the medium, and is of the order of $10^{13} - 10^{14} W/cm^2$ for $\lambda = 10\mu m$. The magnitude of I_{th} is not very sensitive to pulse duration nor gas

pressure. Because the ionization potential of any atom is many times larger than the $10-\mu m$ radiation quantum, multiphoton ionization is least likely to occur with CO_2 laser light, and the tunneling process tends to prevail during strong irradiation.

Another mechanism that causes gas breakdown is cascade (avalanche) ionization where the free electron acquires energy from the laser electromagnetic wave via elastic collisions with neutral atoms. After several collisions it may obtain enough energy to ionize the atom and create a second generation free electron. We discuss below the case for cascade ionization that requires only relatively low levels of laser irradiation, which forms the basis for our proposed scheme.

To initiate the avalanche, the existence of primary free electrons is necessary. We assume that the primary free electrons are uniformly distributed and are produced by using any conventional ionization technique: e.g., corona discharge, UV-light, x-rays, or electron beams. Those exposed to the laser electromagnetic field will oscillate at the laser frequency. The energy of such an osillator, called the pondermotive potential, is equal to

$$\varepsilon = \frac{e^2 E^2}{2 m_e \omega^2}. \tag{9}$$

Energy accumulation by the electron is possible via elastic collisions with neutral molecules, where the kinetic energy of the osillating motion is transferred into longitudinal motion of the electron. The average electron energy increment per collision is $\varepsilon/2$, and the growth rate of the electron kinetic energy ε, under the influence of the electromagnetic wave is

$$\frac{d\varepsilon}{dt} = \frac{\varepsilon \nu_{eff}}{2}$$

where $\nu_{eff} = N_M \nu \sigma$ is the effective electron-molecule momentum transfer collision frequency.

For ionization, energy and momentum conservation require:

$$\frac{N_e d\varepsilon}{dt} \approx \frac{2 E_i d N_e}{dt}$$

Hence, the plasma density growth rate is

$$ln \frac{N_e(t)}{N_e(0)} = \frac{\varepsilon \nu_{eff} t}{4 E_i}. \tag{10}$$

We see from Eqs.(9) and (10) that the characteristic rate of plasma formation depends quadraticaly upon ω. This means that using a CO_2 laser, 100 times less intensity is required to produce the same avalanche ionization effect as compared with a Nd laser. Note that according to the similarity principle, Eqs.(9) and (10) are also applicable to DC fields after replacing ω by ν_{eff}.

It is easy to see that creating a plasma waveguide requires more than just the presence of the laser beam. By comparing Eqs.(5) and (8) we see that the conditions are nearly identical for reflection of a Gaussian beam with a waist w_0 and of an axicon-focused beam used to generate a J_1 plasma profile with $r_{max} = w_0$. That means that the axicon-focused beam will be refracted and even reflected by the laser-produced plasma before waveguide conditions are reached. A possible solution to this problem is to use an additional external electric field. Such a fast turned-on, above-breakdown, DC electric field started prior to the laser pulse will produce a uniform plasma. Then, the laser pulse applied on top of the DC field will produce a J_1-type spatial modulation of the electron density. However, the absolute amplitude of the plasma density modulation, ΔN_e, at the moment of the laser pulse termination is chosen to be well below the magnitude required for waveguiding or reflection of the axicon-focused beam. After the laser pulse termination, the continuing exponential growth of the plasma density under the DC field brings ΔN_e ultimately to the value required for a waveguiding. The laser beam to be guided will be injected inside the plasma channel before total breakdown of the gas occurs.

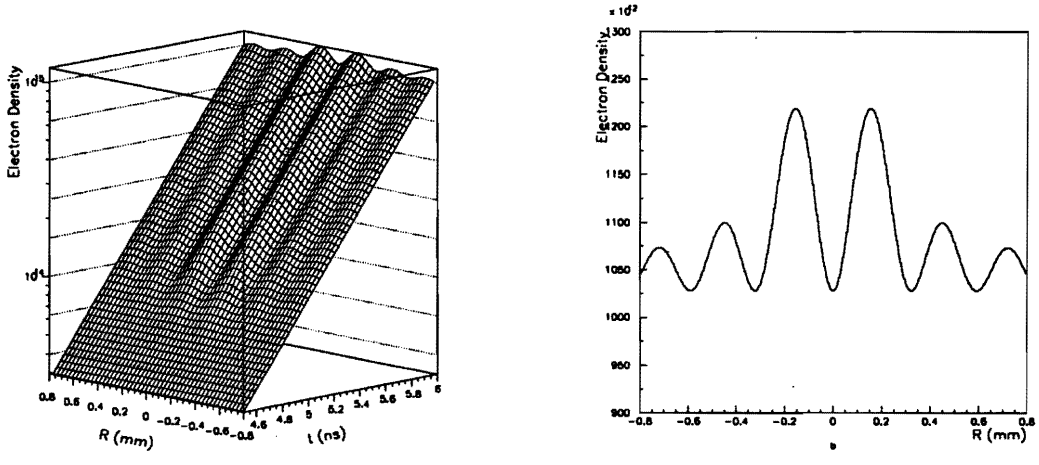

Figure 7: Plasma channel development in DC/laser avalanche. a) dynamics of plasma density profile; b) radial plasma density distribution at t=6 ns. H_2 pressure 0.17 atm; DC(RF) field 8.2 kV/cm; CO_2 laser peak intensity 1 GW/cm^2, Gaussian pulse $I(t) = I(0)exp\{-(2t/\tau)^2\}$ with $\tau = 350ps$, reaches maximum at $t = 5ns$, $N_e(0) = 10^9 cm^{-3}$.

A final condition must also be satisfied: the spatial modulation of the plasma density produced by the J_1 laser beam and enhanced by the DC field should not be washed out by diffusion before the guided beam is injected into the waveguide. Under the DC electric field with the above breakdown amplitude, the major process of plasma channel distortion is electron drift with a velocity of

$$V = \mu E, \tag{11}$$

where μ is the electron mobility, which is inversely proportional to gas pressure.[12] Comparing Eqs.(10) and (11), we see that plasma density growth depends much stronger upon the DC field amplitude than the electron drift. This means there should always be a high enough field to produce a waveguide plasma profile faster than it is distorted by electron drift. Theimpact of the electron drift may be further reduced if the electric field is directed along the axicon axis. An example of such a situation is an accelerating microwave field in a linac cavity. We assume, therefore, that the distortion of the plasma channel due to electron drift or thermal diffusion has a characteristic time much longer than the time interval for the waveguide development measured from the beginning of the laser pulse.

Computer simulations for the plasma waveguide development in 0.17 atm of hydrogen gas made according to Eqs.(7) and (10) are illustrated in Fig. 7. The 8.2 kV/cm strength of the DC or microwave electric field is chosen to produce a 10-times electron multiplication in a 1-ns time interval. The axicon-focused CO_2 laser beam with a Gaussian temporal pulse shape of 350-ps duration produces a 2-time electron multiplication in the first maximum of its J_1 radial Bessel distribution where the peak intensity is equal to 1 GW/cm^2. It should be understood that the preceding parameters were chosen as way of illustration and may be varied depending upon the particular application requirements and other practical considerations.

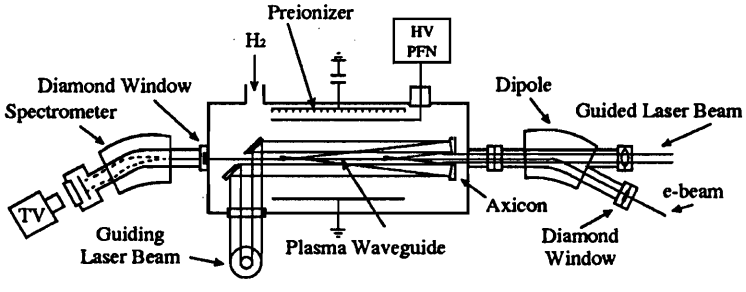

Figure 8: Principal diagram for Plasma Waveguide/Laser Accelerator experiment.

4. Closing

Figure 8 illustrates a possible scheme to demostrate the plasma waveguide which may also be amenable to laser-driven electron acceleration. As was pointed out above, the electrode configuration for a transverse discharge may be replaced by a RF cavity and a coupling waveguide, where a longitudinal microwave electric field is used to produce gas breakdown. Diamond windows separate the gas cell from the evacuated electron-beam line. A UV spark array, x-ray tube, or electron gun may be used as preionizers. Another option for preionization is the column of secondary electrons produced by the preceding electron bunch (e.g. 12-24 ns in advance).

Tests could be performed at the ATF using the existing Inverse Cherenkov Acceleration experiment already equipped with high-power picosecond CO_2 and Nd:YAG lasers, a radial polarization converter, an in-gas axicon focusing system, a $50MeV$ linac, and electron spectrometer.

References

1. A. Ogata, "Laser Wakefield Acceleration Experiments Using a ~1ps $10TW$ Nd: Glass Laser", presented at 6th Workshop on Advanced Accelerator Concepts, June 12-18, 1994, Fontana, WI.
2. O.E. Clayton, K.A. Marsh, M. Everett, A. Lal, and C. Joshi, Proc. of Particle Accelerators Conference, May 17-21, 1993, Washington, DC, p. 2551 (1993).
3. N.A. Ebrahim (Chalk River Laboratories), Private communication.
4. M. Perry, "High Peak Power Lasers", presented at 6th Workshop on Advanced Accelerator Concepts, June 12-18, 1994, Fontana, WI.
5. P. Sprangle, et.al., IEEE Trans. on Plasma Science, PS-15, p. 1451 (1987).
6. P. Sprangle, E. Esarey, J. Krall, G. Joyce, and A. Ting, 5th Workshop on Advanced Accelerator Concepts, AIP Conf. Proc., **279**, p. 490 (1993).
7. T. Katsouleas, T.C. Chiou, C. Decker, W.B. Mori, J.S. Wurtele, G. Shvets, J.J. Su, 5th Workshop on Advanced Accelerator Concepts, AIP Conf. Proc., 279, p. 480 (1993).
8. C.G. Durfee III and H.M. Milchberg, Phys. Rev. Lett., **71**, p. 2409 (1993).
9. J.R. Fontana and R.H. Pantell, J. Appl. Phys. **54**, p. 4285 (1983).
10. S.C. Tidwell, G.H. Kim, and W.D. Kimura, Appl. Opt., **32**, p. 5222 (1993).
11. W.D. Kimura, L. Steinhauer, G.H. Kim, S.C. Tidwell, I. Pogorelsky, K.P. Kusche, Proc. of Particle Accelerators Conference, May 17-21, 1993, Washington, DC, p. 2564 (1993).
12. J.L. Delcoix, "Plasma Physics", V. 2, John Wiley & Sons, London, 1968.